

Supporting Information

Kim et al. 10.1073/pnas.1009926107

SI Materials and Methods

Animals and Surgery. All mice were housed in an animal facility with a specific pathogen-free barrier and experienced a 12-h light-dark cycle. Mice were supplied food and water ad libitum. *Nox2*^{-/-} (*gp91*^{phox-/-}) and *CX₃CR₁*^{+/*GFP*} mice with a C57BL/6 background were purchased from Jackson Laboratories. WT (C57BL/6), *CX₃CR₁*^{+/*GFP*} and *Nox2*^{-/-} male mice aged 8–10 wk and weighing between 23 and 25 g were used for experimentation. For SNT surgery, mice were anesthetized with pentobarbital sodium (50 mg/kg, i.p.). The L5 spinal nerve was transected as previously described, with minor modifications (1). Briefly, an incision was made to the skin from spinal processes at L4 to S2 levels. The paraspinal muscles were separated, and the L6 transverse process was partially removed. After the L5 spinal nerve was separated and transected, the wound was irrigated with saline and closed in two layers with surgical staples. In test mice, drugs were administered before or after surgery. All animal experiment procedures were reviewed and approved by the Institutional Animal Care and Use Committee, Seoul National University. Animal treatments were performed according to the guidelines of the International Association for the Study of Pain.

Behavioral Analysis. Measurement of foot withdrawal thresholds for the contralateral and ipsilateral hind paws was used to assess mechanical allodynia. A 50% withdrawal threshold was measured using a set of von Frey filaments (0.02–6 g, Stoelting), following a modified up-down method (2). Heat hyperalgesia was determined using plantar test instruments (7370; Ugo Basile), following a modified method of Hargreaves et al. (3). A radiant heat source beneath a glass floor was aimed at the plantar surface of the mouse hindpaw. Tests were performed five times for each paw, with a 5-min interval between consecutive tests. Mice were tested for their baseline response twice before surgery. All behavioral tests were performed blinded.

Drug Administration. For intrathecal (i.t.) drug administration, mice were injected under sodium pentobarbital anesthesia (50 mg/kg, i.p.) by direct lumbar puncture between L5 and L6 vertebrae of the spine, using a 10- μ L Hamilton syringe (Hamilton Bonaduz AG) with a 30G 1/2" needle, as previously described (4). Sulforaphane (Calbiochem) stock solution was prepared in DMSO (Sigma) and diluted in PBS just before use. To test the effects on neuropathic pain, sulforaphane (10 mg/kg, 5 μ L total volume in 3% DMSO) was i.t. injected 5 min before SNT. For postoperative treatment, sulforaphane (50 mg/kg in 10% corn oil; Sigma) was injected i.p. at 1 h and 7 d after L5 SNT. DMSO (3% DMSO in PBS, 5 μ L, for i.t. injection) and corn oil (10% corn oil in PBS, 100 μ L, for i.p. injection) served as the vehicle controls. For HO-1 inhibition, tin protoporphyrin (SnPP, Tocris) was introduced twice by i.p. injection (50 μ mol/kg, 5% DMSO in PBS). The first injection was performed with or without sulforaphane (50 mg/kg in 10% corn oil in PBS, i.p.) at 1 h after SNT, and the second injection was administered for SnPP alone at 2 d after surgery.

Detection of Superoxide Using Hydroethidine. Superoxide production after SNT was measured using hydroethidine (Invitrogen), as previously described (5), with minor modifications. At 1 and 3 d after surgery, *CX₃CR₁*^{+/*GFP*} mice were injected i.p. with 100 μ L hydroethidine (1 mg/mL). After 4 h, the animals were treated with sodium pentobarbital (50 mg/kg, i.p.) and killed by transcardial perfusion with 0.9% saline and 200 mL 4% paraformaldehyde (PFA) in PBS. The spinal cord was removed from each mouse and

postfixed for 6 h in 4% PFA. The spinal cord was dehydrated in a 30% sucrose solution for 12 h, and sectioned into 20- μ m-thick slices using a cryocut microtome (Leica CM3050S). Spinal cord sections were placed on gelatin-coated slide glass and were mounted with Vector shield mounting medium (Vector Laboratories). Fluorescent images were captured using a confocal microscope (LSM 5 Pascal; Carl Zeiss).

Primary Spinal Cord Microglia Culture. Primary rat spinal cord microglia were prepared from 7-d-old Sprague-Dawley rats, as previously described (6), with the following minor modifications. Briefly, 7-d-old rats were anesthetized, and the spinal cord was removed. After removal of the meninges, the spinal cord tissue was mechanically disrupted by triturating with a 30-mL syringe and 19-gauge, 1/2-in needle and then seeded into 75-cm² flasks. Cells were cultured in DMEM supplemented with 10% FBS, 1 mM HEPES, 2 mM glutamine, and 1 \times antibiotic/antimycotic (Gibco). Cultures were maintained at 37 °C with 5% CO₂, and the media were changed every 5 d with fresh media containing 5% FBS. After 2 wk, the cells were harvested by gently shaking at 200 rpm for 3 h on an orbital shaker. Microglia were collected from the flasks and were plated in glial culture media. After 30 min, the dishes were washed with fresh medium to remove unattached astrocytes. The resulting cells were found to be >98% microglia by staining with rabbit anti-Iba-1 antibody (1:2,000; Wako).

Immunohistochemistry. Mice were deeply anesthetized with sodium pentobarbital (50 mg/kg, i.p.) and perfused transcardially with 4% PFA in 0.1 M phosphate buffer (pH 7.4). The spinal cord was removed by laminectomy, postfixed at 4 °C overnight, and transferred to 30% sucrose in PBS for 48 h. Spinal cord transverse sections (14- μ m thick) were prepared on gelatin-coated slide glass using a cryocut microtome. The sections were blocked in solution containing 5% normal donkey serum (Jackson ImmunoResearch, Bar Harbor, ME, USA), 2% BSA (Sigma) and 0.1% Triton X-100 (Sigma) for 1 h at room temperature. The sections were then incubated overnight at 4 °C with primary antibody for rabbit anti-Iba-1 (1:2,000, Wako), rabbit anti-GFAP (1:10,000, DAKO), mouse anti-Nox2/*gp91*phox (1:100, Santa Cruz Biotechnology), rabbit anti-HO-1 (1:1,000, Stressgen), mouse anti-8-OHG (1:200, Abcam), rabbit anti-MAP2 (1:2,000, Millipore), rabbit anti-NG2 (1:200, Chemicon), and rat anti-CD11b (1:200, Serotec). The sections were then incubated for 1 h at room temperature with a mixture of FITC-conjugated and Cy3-conjugated secondary antibodies (1:200, Jackson ImmunoResearch). The sections were mounted, and fluorescent images were obtained using a confocal microscope as described. Fluorescent signal intensity was quantified using ImageJ software (National Institutes of Health, Bethesda, MD), as described elsewhere (7).

ELISA. Total protein was prepared from L5 spinal cord tissue or microglia using RIPA buffer (50 mM Tris-HCl, 150 mM NaCl, 1% SDS, 1% Nonidet P-40, 0.5% sodium deoxycholate, 20 mM EGTA) containing protease inhibitors (Calbiochem). Whole-cell/tissue lysates were then collected, and protein concentration was measured using the BioRad protein assay kit (BioRad). TNF- α and IL-1 β protein levels were quantified using mouse TNF- α , mouse-IL-1 β , rat TNF- α , and rat IL-1 β ELISA kits (BioSource) according to the manufacturer's instructions.

Western Blot Assay. To detect nuclear translocation of Nrf2 protein by sulforaphane, cytosolic and nucleic lysates were prepared from pooled L5 spinal cord tissues (*n* = 5) at 6 h postinjury with or

without i.t. sulforaphane injection. To obtain nucleic lysates, spinal cord tissue was homogenized in ice-cold hypotonic lysis buffer (10 mM Hepes, pH 7.9, 10 mM KCl, 0.1 mM EDTA, 1 mM DTT, and 0.2% Nonidet P-40) containing proteinase inhibitors and centrifuged at 4 °C. Pellets were resuspended in ice-cold, hypertonic, nuclear extract buffer (20 mM Hepes pH 7.9, 0.4 M NaCl, 1 mM EDTA, 1 mM DTT), containing proteinase inhibitors. Total protein concentration of each sample was measured using the BioRad protein assay kit. A total of 40 µg tissue or cell lysate from each sample was resolved by electrophoresis on a 10% SDS/PAGE gel. Proteins were transferred to nitrocellulose membranes and blocked with Tris-buffered saline containing 5% nonfat dry milk and 0.1% Tween-20. The membranes were probed with rabbit anti-Nrf2 antibody (1:100, Santa Cruz Biotechnology) at 4 °C overnight, followed by incubation with HRP-conjugated secondary antibody at room temperature for 1 h before ECL (GE Healthcare Bio-Sciences) treatment and exposure to x-ray film. The membranes were stripped and reprobed with goat anti-Lamin B (1:200, Santa Cruz Biotechnology) and rabbit anti-β-actin (1:1,000, Sigma) antibodies.

Ipsilateral L5 hemispinal cord tissues were removed from 0.9% saline-perfused mice. The tissues ($n = 4$, each time point) were pooled and washed twice in ice-cold PBS and homogenized using

a micro tissue grinder (Wheaton) in 200 µL RIPA buffer (50 mM Tris-HCl, 150 mM NaCl, 1% SDS, 1% Nonidet P-40, 0.5% sodium deoxycholate, 20 mM EGTA) containing protease inhibitors (Calbiochem). Tissue lysate (40 µg) from each sample was resolved by electrophoresis on a 10% SDS/PAGE gel. The proteins were transferred to nitrocellulose membranes and probed with antibody for mouse anti-Nox2/gp91phox (1:100, Santa Cruz Biotechnology) antibody overnight at 4 °C, followed by incubation with HRP-conjugated secondary antibody at room temperature for 1 h and ECL detection. The membranes were stripped and reprobed with rabbit anti-β actin (1:1,000, Sigma) antibodies.

Real-Time RT-PCR. Total RNA from isolated L5 spinal cord tissue and cells was extracted using TRIzol reagent (Invitrogen), and reverse transcribed using M-MLV Reverse Transcriptase (Invitrogen). Real-time PCR was performed using a 7500 Real-Time PCR system (Applied Biosystems). Relative mRNA levels were calculated according to the $2^{-\Delta\Delta C_t}$ method (8). All ΔC_t values were normalized to GAPDH. All real-time RT-PCR experiments were performed at least three times, and the mean \pm SEM values were presented unless otherwise noted. The PCR primer sequences used in this study are listed in [Tables S1](#) and [S2](#).

1. Tanga FY, Nutile-McMenemy N, DeLeo JA (2005) The CNS role of Toll-like receptor 4 in innate neuroimmunity and painful neuropathy. *Proc Natl Acad Sci USA* 102: 5856–5861.
2. Chaplan SR, Bach FW, Pogrel JW, Chung JM, Yaksh TL (1994) Quantitative assessment of tactile allodynia in the rat paw. *J Neurosci Methods* 53:55–63.
3. Hargreaves K, Dubner R, Brown F, Flores C, Joris J (1988) A new and sensitive method for measuring thermal nociception in cutaneous hyperalgesia. *Pain* 32:77–88.
4. Hylden JL, Wilcox GL (1980) Intrathecal morphine in mice: A new technique. *Eur J Pharmacol* 67:313–316.
5. Lewén A, Sugawara T, Gasche Y, Fujimura M, Chan PH (2001) Oxidative cellular damage and the reduction of APE/Ref-1 expression after experimental traumatic brain injury. *Neurobiol Dis* 8:380–390.
6. Kim D, et al. (2007) A critical role of toll-like receptor 2 in nerve injury-induced spinal cord glial cell activation and pain hypersensitivity. *J Biol Chem* 282:14975–14983.
7. Xu M, Bruchas MR, Ippolito DL, Gendron L, Chavkin C (2007) Sciatic nerve ligation-induced proliferation of spinal cord astrocytes is mediated by kappa opioid activation of p38 mitogen-activated protein kinase. *J Neurosci* 27:2570–2581.
8. Livak KJ, Schmittgen TD (2001) Analysis of relative gene expression data using real-time quantitative PCR and the $2^{-\Delta\Delta C(T)}$ Method. *Methods* 25:402–408.

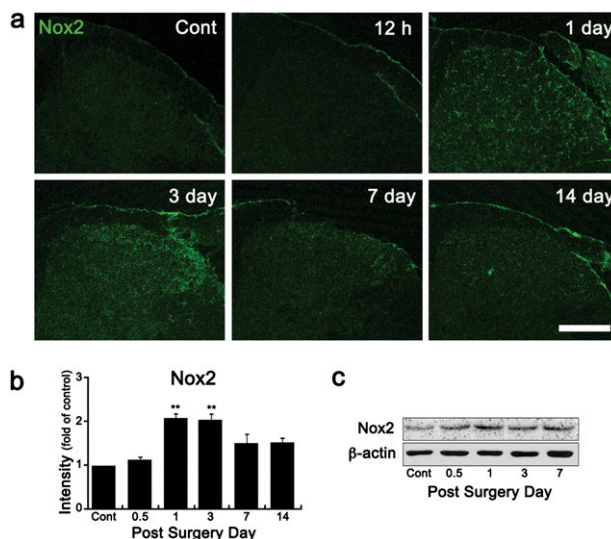


Fig. S1. Nox2 is up-regulated in the ipsilateral dorsal horn after SNT. (A) Nox2 expression was tested in ipsilateral L5 dorsal horns at various time points after SNT by immunostaining with anti-Nox2/gp91phox antibody. (Scale bar, 200 µm.) (B) The fluorescent intensity of Nox2 signals were measured and presented in fold-increase compared with the level of control ($*P < 0.05$; $**P < 0.01$). (C) Nox2 expression was measured by Western blot assay using pooled ipsilateral L5 hemispinal cord tissues of uninjured and SNT-injured mice (each group, $n = 4$). A representative picture is shown.

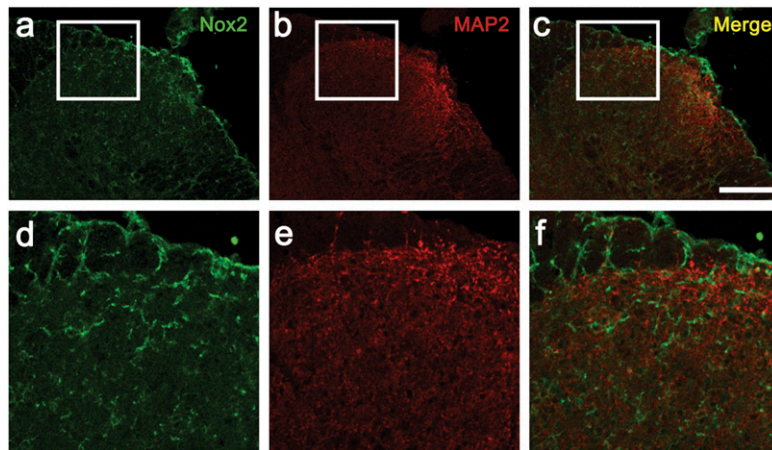


Fig. 52. Nox2 expression was not detected in spinal dorsal horn neurons. Spinal cord sections of SNT-injured mice 1 d postsurgery were stained with anti-Nox2 (green) and anti-MAP2 (red) antibodies. (Scale bar, 200 μm .)

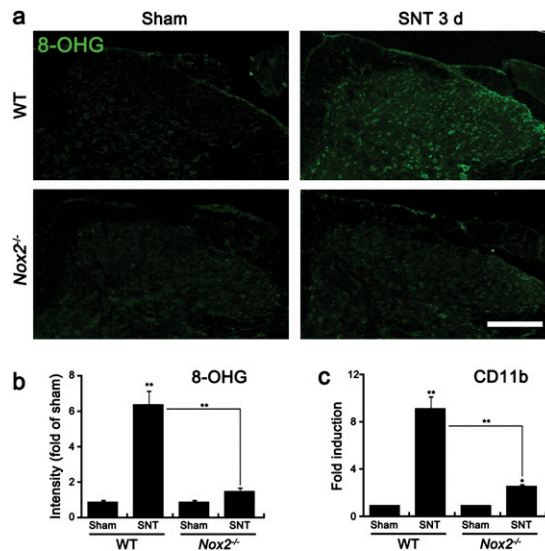


Fig. 53. SNT-mediated ROS damage and microglia activation in the spinal cord were reduced in $Nox2^{-/-}$ mice. (A) ROS-induced cellular damage was tested using 8-OHG immunostaining in the ipsilateral L5 dorsal horn of WT ($n = 4$) and $Nox2^{-/-}$ ($n = 4$) mice at 3 d postsurgery. (Scale bar, 200 μm .) (B) Fluorescent intensities of 8-OHG signals were measured and presented as fold-increase compared with levels in the sham-control sample. (C) Total RNA was prepared from L5 spinal cord of WT (WT-SNT, $n = 4$) and $Nox2^{-/-}$ ($Nox2^{-/-}$ -SNT, $n = 4$) mice at 3 d after SNT, and used for real-time RT-PCR to detect CD11b transcripts. Levels of CD11b in SNT-injured mice were normalized to the level of sham control mice (Sham, $n = 4$) and presented as fold-induction. (* $P < 0.05$; ** $P < 0.01$).

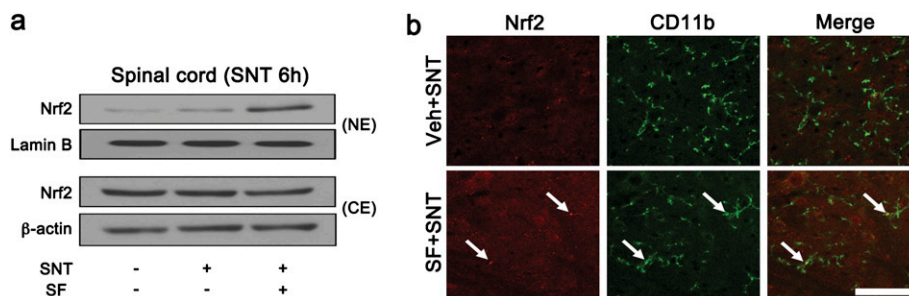


Fig. 54. Administration of sulforaphane induces nuclear translocation of Nrf2 in spinal cord microglia. (A) Nuclear (NE) and cytosolic extracts (CE) were prepared from pooled ipsilateral L5 hemispinal cord tissues of sham-operated ($n = 5$) or SNT-injured ($n = 5$) mice with vehicle or sulforaphane-injection (10 mg/kg, in 3% DMSO, i.t.), and used in Western blot assays to detect Nrf-2. Antibodies for Lamin B and β -actin were used to verify nuclear and cytoplasmic fractions, respectively. Sulforaphane injection increased Nrf-2 levels in the nuclear fraction. (B) Nrf-2-expressing cell types were investigated by immunohistochemistry. Nrf-2 signal was detected in spinal cord tissues of sulforaphane-injected mice at 6 h post-SNT injury. The Nrf-2 signal was colocalized to the CD11b immunoreactive microglia.

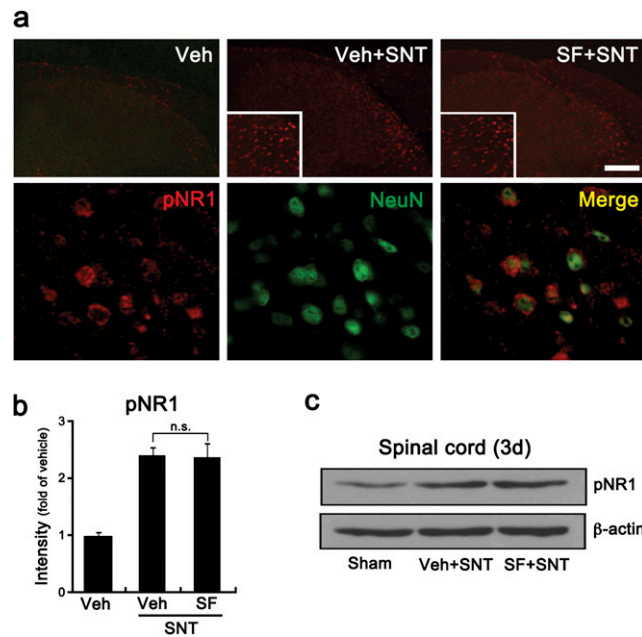


Fig. 55. Sulforaphane does not affect SNT-induced NR-1 phosphorylation. (A) L5 spinal cords of sham-operated, vehicle-injected mice (Veh, $n = 3$), SNT-injured vehicle-injected mice (Veh+SNT, $n = 6$), and SNT-injured sulforaphane-injected mice (SF+SNT, $n = 6$) were stained with anti-pNR1 (red) and anti-NeuN (green) antibodies at 3 d postsurgery. pNR1 was detected only in NeuN⁺ neurons. (B) Fluorescence intensity of pNR1 signals was quantified and presented in fold-increase compared with the level of control. n.s., not significant. (C) Levels of pNR1 in the spinal cord of sham-operated, SNT-injured vehicle-injected, and SNT-injured sulforaphane-injected mice were measured by Western blot analysis.

Table S1. Primer sequences used for real-time RT-PCR

Gene	Forward primer	Reverse primer	GenBank no.
Mouse <i>GAPDH</i>	5'-AGG TCA TCC CAG AGC TGA ACG-3'	5'-CAC CCT GTT GCT GTA GCC GTA T-3'	NM_008084
Mouse <i>CD-11b</i>	5'-TAA TGA CTC TGC GTT TGC CCT G-3'	5'-TAA TGA CTC TGC GTT TGC CCT G-3'	NM_008401
Mouse <i>GFAP</i>	5'-TCA ACG TTA AGC TAG CCC TGG A-3'	5'-CGG ATC TGG AGG TTG GAG AAA G-3'	NM_010277
Mouse <i>TNF-α</i>	5'-AGC AAA CCA CCA AGT GGA GGA-3'	5'-GCT GGC ACC ACT AGT TGG TTG T-3'	NM_013693
Mouse <i>IL-1β</i>	5'-TTG TGG CTG TGG AGA AGC TGT-3'	5'-AAC GTC ACA CAC CAG CAG GTT-3'	NM_008361
Mouse <i>HO-1</i>	5'-TCA CAG ATG GCG TCA CTT CGT-3'	5'-TGT TGC CAA CAG GAA GCT GAT-3'	NM_010442
Mouse <i>Nox2</i>	5'-GAC CCA GAT GCA GGA AAG GAA-3'	5'-TCA TGG TGC ACA GCA AAG TGA T-3'	U43384
Rat <i>TNF-α</i>	5'-TAG TCG GTC CCA CAC AGG A-3'	5'-TGC TTG GTG GTT TGC TAC GA-3'	AY427675
Rat <i>IL-1β</i>	5'-TGC TGA TGT ACC AGT TGG GG-3'	5'-CTC CAT GAG CTT TGT ACA AG-3'	NM_031512

Table S2. Primer sequences used for RT-PCR

Gene	Forward primer	Reverse primer	GenBank no.
Mouse <i>GAPDH</i>	5'-AGG TCA TCC CAG AGC TGA ACG-3'	5'-CAC CCT GTT GCT GTA GCC GTA T-3'	NM_008084
Mouse <i>Nox1</i>	5'-ACA GAG GAG AGC TTG GGT GA-3'	5'-CAC TCC AGG AAG GAA ATG GA-3'	NM_172203
Mouse <i>Nox2</i>	5'-GCT GGG ATC ACA GGA ATT GT-3'	5'-GGT GAT GAC CAC CTT TTG CT-3'	U43384
Mouse <i>Nox3</i>	5'-GCA CCG GGA CAG TAC ATC TT-3'	5'-AGT GAC TCC AAT TCC CGT TG-3'	BC106862
Mouse <i>Nox4</i>	5'-TGT TGC ATG TTT CAG GTG GT -3'	5'-TGG AAC TTG GGT TCT TCC AG -3'	BC138918
Mouse <i>Duox1</i>	5'-TTC CCC TTA GTC AGC CTC CT-3'	5'-GAG CCT GCC ATC CAC TAC TC-3'	NM_001099297
Mouse <i>Duox2</i>	5'-AGT GTG CGC CTG TTA CTG TG-3'	5'-AAC CGT TTG TCA AGG ACC TG-3'	NM_177610